

Design and Parametric Weight Optimization of Four Wheeler Lower Control Arm

M. Balaji Rao¹, J.A. Sandeep Kumar², A.V. Hari Babu³

M.Tech., (PG Scholar), Dept. of ME, SVR Engineering College, Nandyal, India¹

Assistant Professor, Dept. of ME, SVR Engineering College, Nandyal, India²

Associate Professor, Dept. of ME, SVR Engineering College, Nandyal, India³

ABSTRACT: Suspension system of an automobile plays an important role in ensuring the stability of the automobile. Another major aspect of suspension system in passenger cars is luxury. A lot of research is going on in this direction, to further the development of independent suspension systems for automobiles. In the independent suspension system the control arm plays a major role. It is generally made of forged steel but this material is found to be excessively heavy in the current context of the quest for reducing the weight of the automobiles without any significant changes to design. In this task of designing the control arms with alternative materials, Computer Aided Engineering (CAE) software being extensively used to perform the topology optimization. The main objective of this study is to reduce the weight of the lower control arm of independent suspension by using topology optimization and material optimization. Static loads were taken into consideration and analysis is done for two different models viz. the existing model and an optimized model developed by topology optimization. Static structural analysis & modal analysis of lower control arm is carried out by using HYPERWORKS. The obtained results of existing model are compared with the optimized model and their weights are calculated for two different materials. The best model from this study is proposed based on the topology and material optimization.

I.INTRODUCTION

In automobiles, a double wishbone suspension is an independent suspension design using two wishbone-shaped arms to support the wheel as shown in Fig 1.1. Double wishbones provide more stability to wheel movements at high speeds which reduces camber angle as the wheel moves up and down over uneven surfaces. Wishbones can be very easily adjusted as every joint can be removed for optimal wheel movement. During the actual working conditions, the maximum load is transferred from upper wishbone arm to the lower arm which may cause failure and bending of lower wishbone arm either at the ball joint location or at control arm because of high impact loads that are could be produced by road conditions. Such failure should be avoided to ensure the reliability of the suspension system and the automobile.

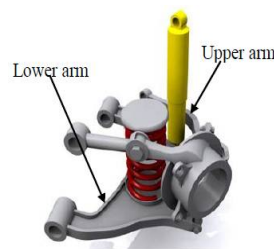


Fig1.1: suspension system

Double wishbone suspension system is one type of independent suspension system which consists of two lateral control arms namely upper and lower arm. The control arm is nearly flat and roughly triangular member that pivots in two places. The broad end of triangle is attached at the frame and pivots on bushing. The Lower control arm is also called as

International Journal of Innovative Research in Science, Engineering and Technology

(An ISO 3297: 2007 Certified Organization)

Website: www.ijirset.com

Vol. 6, Issue 6, June 2017

A-arm. Control arms can be used in an all-wheel independent suspension system. During running condition lower control arm is subjected to loads due to variation in gross weight and impact loads due to fluctuation of road surface and additional forces such as braking and cornering. Because of this complex nature of loads, the chances of bending and hence failing of lower control arm at ball joint are very high which is undesirable. The lower control arm is one of the major parts of the front suspension system which controls the wheel trace and transmits the load on the wheel by the road to other parts of the car. It is assembled between the wheel hub and the automobile chassis as shown in Fig 1.2. When the car runs on the road, the lower control arm is subjected to complex loads that constantly change with time. Thus, the mechanical performance, usually relating to strength and stiffness are critical to the safety and reliability of the car.



Fig1.2: Assembly of suspension system

The main functions of control arm are:

- To form a rigid connection between the chassis and wheel hub, to which wheel is attached.
- To allow the wheel, the required degrees of freedom for proper steering and suspension abilities.
- To support the spring and dampers, which form the major components for shock absorbing.
- To do these functions properly the control arm needs to be sufficiently strong. Depending upon the position of the control arm, there are mainly two types of control arms Upper and lower control arm. The springs and shock absorbers are supported between these arms.

II.RELATED WORK

In automotive industry simulation-based improvement of models has been used for a variety of applications. In the study of XueGuanSong et al.(2010), based on the FEM analysis, both the response surface model(RSM)and Kriging model are used to optimize an ADI upper control arm, where the weight of the upper control arm is considered as the design objective, and the maximum allowable vonmises stress is the constraint objective. The initial FEM analysis shows the stress distribution and maximum stress on the upper control arm under a very severe loading condition. And, by virtue of the result of FEM analyses, fifty simulations with six design variables are performed for RSM and Kriging model to construct the approximation of the weight and maximum stress to obtain the optimum result. The optimized results obtained by using RSM and KRG are confirmed by a verified FEM analysis. In addition, a fatigue analysis is carried out to verify the durability of the final design.

Suspension system of an automobile plays an important role in ensuring the stability of the automobile. Although it has been achieved to a considerable extent, another major aspect of suspension system in a passenger car is luxury. A lot of research is going on in this direction, which resulted in the development of independent suspension system. Control arm plays a major role in independent suspension system. It is generally made of forged steel which has considerable disadvantages such as weight, cost etc.P.Nagarjuna et al. (2012),presented the development of sheet metal control arm, which has many advantages over forged metal. Stability, road handling and comfort of vehicle depend on optimum design of suspension system. Mostly all passenger cars and light trucks use independent suspension system because of inherent advantages over rigid suspension systems. Double wishbone system which is also called as Short Long Arm system consists of upper and lower wishbone arms. While actual running condition forces like braking, cornering and vertical loads are taken by lower arm of suspension system, hence probability of failure of lower arm under these forces is more.Also this component is subjected to road irregularities, hence its dynamic behaviour need to be understood. The study conducted by Vinayak Kulakarni et al. (2014) deals with calculating the forces acting on lower wishbone arm while vehicle is subjected to critical loading conditions (Braking, Cornering and Descending though slope). Suspension geometry and suitable materials for the suspension arm have been identified. Lower arm suspension has been modelled

International Journal of Innovative Research in Science, Engineering and Technology

(An ISO 3297: 2007 Certified Organization)

Website: www.ijirset.com

Vol. 6, Issue 6, June 2017

using Pro-Engineer. Vonmises stress –strain is carried out in order to find out maximum induced stress and strain, while modal analysis is done for finding out natural frequencies and mode shapes of component are analyzed in the study. These analyses were carried using Altair Hyper works and solver used is Radioss. From the analyzed results, design parameters were compared for two different materials and best one was identified. From result obtained it was found that existing design was safe and was somewhat overdesign. So in order to save material and reduce weight of component, Topology optimization analysis is carried out in Hyper works which yielded in optimized shape. The study of A.S. Todkar et al. (2013), was focused on stress strain analysis of lower control arm. The wishbone control arm is a type of independent suspension used in motor vehicles. The general function of control arms is to keep the wheels of a motor vehicle from uncontrollably changing the direction when the road conditions are not smooth. The control arm suspension normally consists of upper and lower arms. The upper and lower control arms have different structures based on the model and purpose of the vehicle. By many accounts, the lower control arm is the better shock absorber than the upper arm because of its position and load bearing capacities. It has an “A” shape on the bottom known as wishbone shape which carries most of the load from the shock received. The lower control arm takes most of the impact that the road has on the wheels of the motor vehicle. It either stores that impact or sends it to the coils of the suspension depending on its shape. During the actual working condition, the maximum load is transferred from upper wishbone arm to the lower arm which creates possibility of failure in the arm. Similarly, impact loading produces the bending which is not desirable. Hence it is essential to focus on the stress strain analysis study of lower wishbone arm to improve and modify the existing design. The present study will contribute in this problem by using finite element analysis approach.

III. MODELING

The full form of CATIA is computer aided three dimensional interactive applications and it was developed by Dassault system, in France

The CATIA is a powerful CAD/CAE/CAM tool for product life cycle management. It is easy to because of its flexibility and its versatility enables designing of complex geometries as well as quick re-designing of available geometries. And it is also improves the innovative design concepts and gives the best design strategy, better productivity and creativity. It helps in creating the product from concept generation to the final product with in the given span of time with best design. In CATIA, we have different types of workbenches. A workbench means definite environment which involves the set of tools and these tools are utilized to perform the best design within a particular area

Sketcher:

CATIA sketcher tools primarily draft a rough sketch following the shape of the profile. The objects created are converted into a proper

sketch by applying geometric constraints and dimensional constraints. These constraints refine the sketch according to a rule. Adding parametric dimensions further control the shape and size of the feature. Line, rectangle, palette, constrain, dimension modification, and text etc., are used as one of the feature creation tools to convert the sketcher entity into a part feature.

Design of lower control arm

As we know that the lower control arm is very important that and it should have proper stiffness and strength characteristics for the safety of a vehicle, while maintaining light weight. The details of the geometry are taken from the existing component and it is developed by the commercial tool CATIA. After opening the CATIA, one plane is selected and the sketcher workbench is activated to develop 2D model based on the dimensions. After this the sketcher is closed 3D model is created using suitable commands.

International Journal of Innovative Research in Science, Engineering and Technology

(An ISO 3297: 2007 Certified Organization)

Website: www.ijirset.com

Vol. 6, Issue 6, June 2017

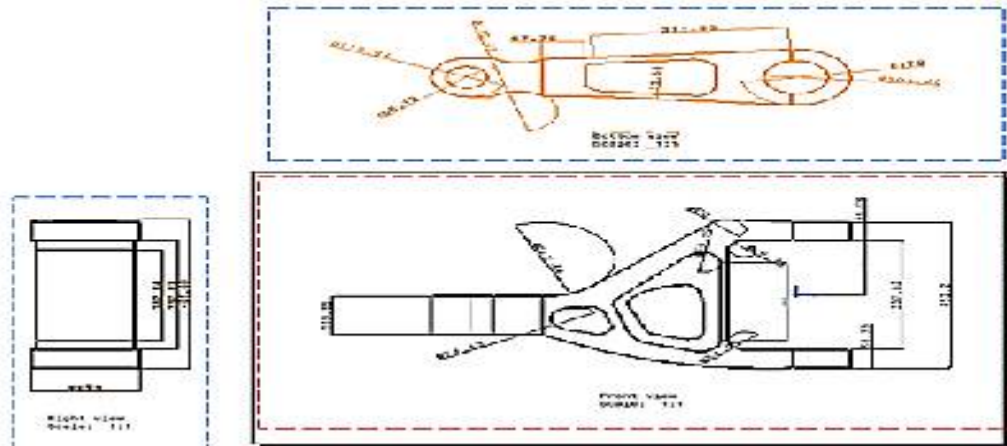


Fig 3.1: draft design of control arm

Before starting the geometric modelling of the lower control arm, the origin is assumed. Based on the origin we can develop 2D sketches of each of the parts of the model in the sketcher as shown in fig 3.1 and with the use of suitable commands convert 2D sketchers into 3D solid components using “EXIT WORKBENCH”.

IV. MESHING

The details of the geometry are taken from an existing component and the 3D model is developed by the commercial tool “CATIA” as described above and the file is saved in step file. After developing the CATIA model, it is exported to HYPERMESH. The figure 4.1 shows the imported file from CATIA. Import the CAD model into Hypermesh V13. File → Import → Geometry → Browse .IGS file → import

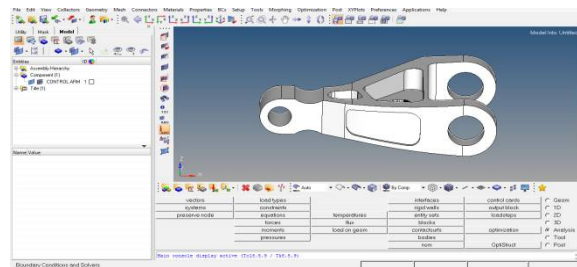


Fig 4.1: Imported geometry in Hypermesh.

4.2 Meshing

Steps involved in meshing of the geometry using Hypermesh are selection of mesh type, meshing method and type of elements used in the mesh as shown in figure 4.2.

Mesh Type: 3D mesh

Mesh Method: Volume Tetra Mesher

Mesh Element: Tetrahedral

Mesh → 3D → Tetra Mesh → Volume Tetra → Element Size → 10 → Mesh

International Journal of Innovative Research in Science, Engineering and Technology

(An ISO 3297: 2007 Certified Organization)

Website: www.ijirset.com

Vol. 6, Issue 6, June 2017

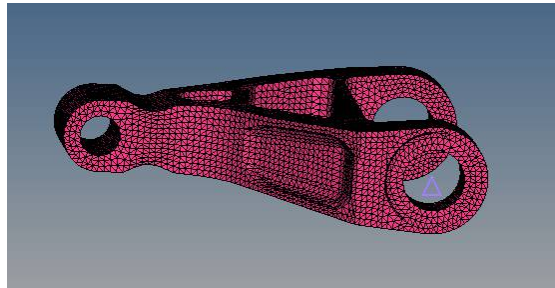


Fig 4.2: Meshing component

Finding Free Edges

In addition to the node connectivity problems, there could also be free edges in the generated mesh. The presence of free edges and T edges between the nodes and elements should thus be checked after meshing. If there are any free edges and T edges on the component, remeshing may be required to eliminate the free edges. The free edges in hypermesh could be found using Shift+F3 option. Free edges are shown in figure 4.3. Tool→ edges→ elements→ displayed→ find edges



Figure 4.3: Free edges of elements

Removing Edges:

If there are any spurious edges that are created these edges are saved into temp file. From the temp file elements related to free edges can be found using shiftF3 and they can be removed. The final component, the control arm with the mesh is shown in figure 4.4.



Figure 4.4: Final meshed model

Elements Checking: If there are no free edges on the component, then it is required to find the failure elements using “tap collapse” option. If there are any failure elements on the component we have to modify them using available options in hypermesh (Split surface line, replace point etc.) to get better results. The tap collapse could be found in hypermesh using Shift+F10 option. To get the quality analysis check the below functions as shown in figure 4.5. Tool→ check elements→ 3D→ warpage→ connectivity→ check. The elements are treated as failed elements if they do not conform to the following criteria: Tet collapse < 0.1 Aspect < 5 Jacobian < 0.7

International Journal of Innovative Research in Science, Engineering and Technology

(An ISO 3297: 2007 Certified Organization)

Website: www.ijirset.com

Vol. 6, Issue 6, June 2017



Figure 4.5: Elements checking in hyper mesh

Calculate the Number of Nodes and Elements

If there are no free edges and no failure elements on the component then the meshing is ready to do analysis. Before that the number of nodes and elements present on the existing model is calculated using tool option. The total number of nodes are shown in figure 4.6

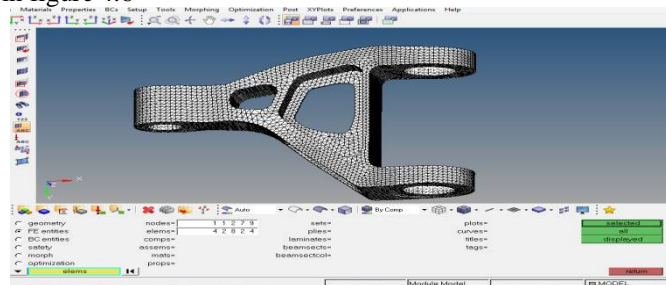


Figure 4.6: No of nodes and elements displayed option in Hypermesh

Number of nodes in the model used here is 11279 and elements are 42824. The quality of total number of elements created is ensured by monitoring the parameters like jacobian, warpage, skew, aspect ratio and connectivity and verifying that they are within acceptable limits.

Dynamic axle loads:

All calculations presented are based on the main assumption that the chassis of the car under consideration is rigid. Calculation of the loads at each wheel in different operating conditions will be discussed for the rest of this section: The vehicle braking on level ground The vehicle at the instant of cornering The vehicle downhill grade The vehicle at the instant of braking on a downhill grade.

International Journal of Innovative Research in Science, Engineering and Technology

(An ISO 3297: 2007 Certified Organization)

Website: www.ijirset.com

Vol. 6, Issue 6, June 2017

CASE :-1.The vehicle braking on level ground :

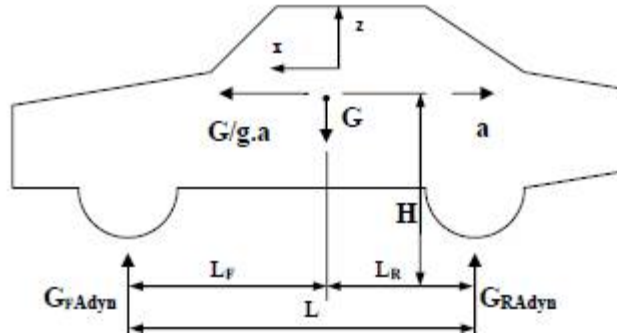


Figure 4.14: Forces acting on a vehicle during braking

The car is under negative acceleration as show in figure 4.13, an inertial reaction force denoted by $(G/g.a)$ acting at the centre of gravity opposite to the direction of the acceleration . During the vehicle decelerates, load is transferred from the rear axle to the front axle.

By considering the equilibrium of moments about the front and rear tire-ground contact points, the normal loads on the front and rear axle are,

$$G_{FAdyn} = \frac{G \cdot L_R + m \cdot a \cdot H}{L}, \frac{(29920.5 \times 1276) + (3050 \times 0.00926 \times 1160)}{2900} = 13176.3172 \text{ N.}$$

$$G_{RA dyn} = \frac{G \cdot L_F - m \cdot a \cdot H}{L}, \frac{(29920.5 \times 1624) - (3050 \times 0.00926 \times 1160)}{2900} = 16744.182 \text{ N}$$

The transferred load to the front axle is found from the following equation

$$GT = G_{FAdyn} - G_{FA}, 13176.3172 - 13165.02 = 11.2972 \text{ N.}$$

Case2: The vehicle at the instant of Cornering:
(Lateral Load Transfer on the Banking)

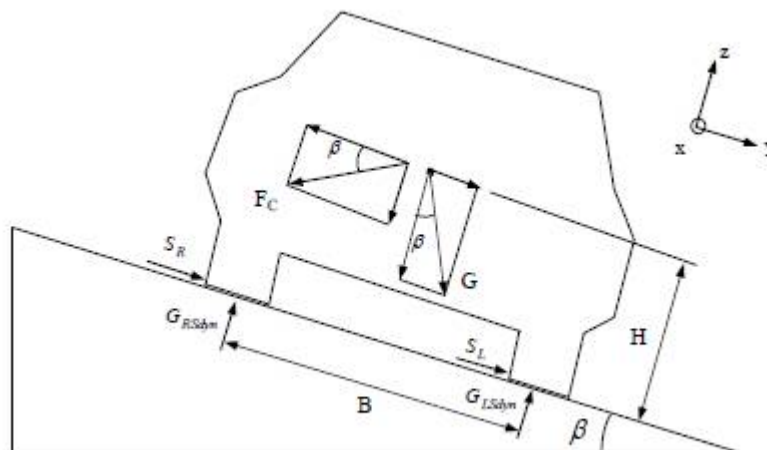


Figure 4.15: Forces acting on a vehicle during cornering

International Journal of Innovative Research in Science, Engineering and Technology

(An ISO 3297: 2007 Certified Organization)

Website: www.ijirset.com

Vol. 6, Issue 6, June 2017

The centrifugal force which results from the speed V , the radius of the bend R and the total weight of the vehicle is;

$$FC = \frac{m.V^2}{R}$$

F_c = Centrifugal force
 V = velocity
 $V = 120 * 100 / 3600 = 33.33 \text{m/sec}$

$$GRS \text{ dyne} = \frac{G}{B} \left[\frac{V^2}{g \times R} \left(H \times \cos \beta + \frac{B}{2} \times \sin \beta \right) + \frac{B}{2} \times \cos \beta - H \sin \beta \right]$$

$$GRS \text{ dyne} = \frac{29920.5}{1.67} \left[\frac{33.33^2}{9.81 \times 100} \left(1.16 \times \cos(0) + \frac{1.67}{2} \times \sin(0) \right) + \frac{1.67}{2} \times \cos 0 - 1.16 \sin(0) \right]$$

$GRS \text{ dyne} = 38495.12982 \text{N}$

$$GLS \text{ dyne} = \frac{G}{B} \left[\frac{V^2}{g \times R} \left(\frac{B}{2} \times \sin \beta - H \times \cos \beta \right) + \frac{B}{2} \times \cos \beta + \sin \beta \right]$$

$$GLS \text{ dyne} = \frac{29920.5}{1.67} \left[\frac{33.33^2}{9.81 \times 100} \left(\frac{1.67}{2} \times \sin(0) - 1.16 \times \cos(0) \right) + \frac{1.67}{2} \times \cos 0 + 1.16 \sin(0) \right]$$

$GLS \text{ dyne} = -8574.629 \text{N}$

Transferred load from the left side to the right side of the vehicle while cornering

$$GC = GRS \text{ dyne} - \frac{G}{2}$$

$$GC = 38495.12982 - \frac{29920.5}{2}$$

$GC = 23534.879 \text{N}$

Case: 3 The vehicle on a Downhill grade

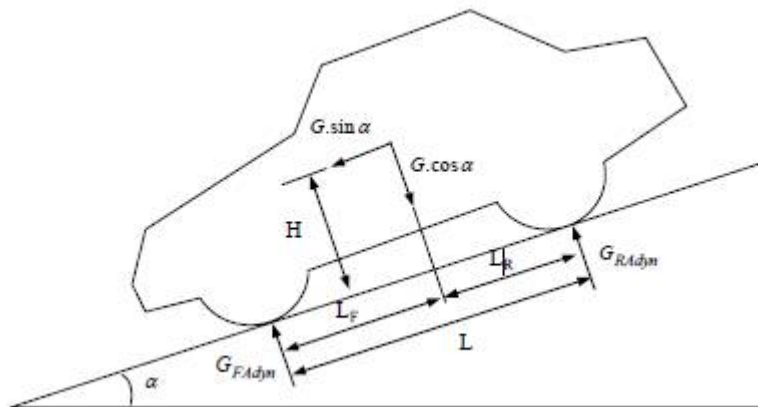


Figure 4.16: Forces acting on a vehicle on a downhill grade

A negative grade causes load to be transferred from the rear to the front axle. On roads, the grade angle occasionally reaches 10 to 12 per cent, The major external direction, the aerodynamic resistance R_a , rolling resistance of the front and rear tires R_{rf} and R_{rr} are neglected for this case,

The dynamic loads on the front and rear axle are determined by summing moments equilibriums

$$GFA \text{ dyne} = \frac{G}{L} (H \cdot \sin \alpha + L_R \cdot \cos \alpha)$$

$$GRA \text{ dyne} = \frac{G}{L} (L_R \cdot \cos \alpha - H \cdot \sin \alpha)$$

International Journal of Innovative Research in Science, Engineering and Technology

(An ISO 3297: 2007 Certified Organization)

Website: www.ijirset.com

Vol. 6, Issue 6, June 2017

$$\text{GFA dyne} = \frac{29920.5}{2.9} (1.16 \cdot \sin(11) + 1.27 \cdot \cos(11)) = 15146.0146\text{N}$$

$$\text{GRA dyne} = \frac{29920.5}{2.9} (1.27 \cdot \cos(11) - 1.16 \cdot \sin(11)) = 14163.99442\text{N}$$

Transferred load from rear axle to front axle is

$$\text{GT} = \text{GFA dyne} - \text{GFA}$$

$$\text{GT} = 15146.0146 - 13165.02$$

$$\text{GT} = 1980.9946\text{N.}$$

Case:4 The vehicle at the instant of braking on a downhill grade

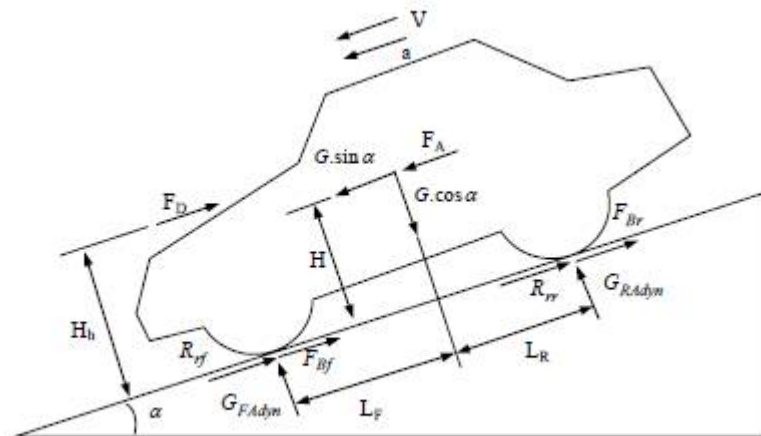


Figure 4.17: Forces acting on a vehicle braking on a downhill grade

The dynamic loads on the front and rear axle are determined by the summing moments equilibriums

$$\text{GFA dyne} = \frac{1}{L} [G \cdot (H \times \sin \alpha + L_R \times \cos \beta) + F_A \times H - F_D \times H_h]$$

$$\text{GFA dyne} = \frac{4.8}{2.9} \left[29920.5 \times (1.16 \times \sin(11) + 1.276 \times \cos(11)) + 28.24 \times 1.16 - 797.30 \times 1.11 \right]$$

$$\text{GFA dyne} = 71290.258\text{N}$$

$$\text{GRA dyne} = \frac{1}{L} [G \cdot (L_F \times \cos \alpha - H \times \sin \alpha) + F_D \times H_h - F_A \times H]$$

$$\text{GRA dyne} = \frac{4.8}{2.9} \left[29920.5 \times (1.624 \times \cos(11) - 1.16 \times \sin(11)) + 797.14117 \times 1.11 - 28.243 \times 1.16 \right]$$

$$\text{GRA dyne} = 69397.4878\text{N.}$$

$$\text{GFAw} = \frac{\text{GFA}}{2} = \frac{71290.2583}{2} = 35645.1291\text{N.}$$

The braking inertia force is:

$$F_A = m \cdot a$$

The aero dynamic forces produced on a vehicle arise from two sources, from (or pressure) drag and rolling resistance of the tires. Drag is the largest and most important aerodynamic force. The aerodynamic drag is

$$F_D = C_D \cdot A \cdot \frac{\rho_a}{2} \cdot V^2$$

$$F_D = 0.32 \cdot 3.482 \cdot \frac{1.288}{2} \cdot 33.332^2$$

$$F_D = 797.14117$$

The drag coefficient, C_D is determined empirically for the car. The frontal area, A is the scale factor taking into account the size of the car. The frontal area of the vehicle in range of 79-84% of a car calculated from the overall vehicle width and height. The frontal area %80 of area is

$$A = 0.80 \cdot b \cdot h,$$

$$A = 0.80 \cdot 1.961 \cdot 2.22$$

$$A = 3.482\text{m}$$

The aerodynamic force is assumed to be acting on the center of the vehicle cross-section area

$$Hh = \frac{h}{2}$$

$$Hh = \frac{2.22}{2}$$

$$Hh = 1.11m$$

The other major vehicle resistance force on level ground is the rolling resistance of the tires by the equation

$$FR = G \cdot fR \cdot \cos\alpha$$

$$FR = 29920.5 * 0.015 * \cos(11)$$

$$FR = 440.561N.$$

Where and are the braking force of the front and rear axles, respectively. The magnitude of the transmission resistance is small and can be neglected in the braking calculations

V. EXPERIMENTAL RESULTS

Static Structural Analysis

Mild steel

Lower control arms are generally made of mild steel due to their high compressive strength, wear resistance, excellent machinability, low cost, etc. First simulation is performed by taking the material of the control arm to be mild steel. The lower control arm behaves like a cantilever beam at the one hole side is fixed and two holes side is free. From the fig6.1 it is clear that maximum displacement occurs at the free end.

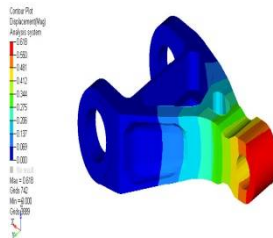


Figure 5.1: Displacement for mild steel reference design

Based on the given loading conditions the model behaves like a cantilever beam. For cantilever beam the maximum bending stresses is developed at fixed support. The von Mises stress distribution of mild steel of lower control arm is shown in the figure6.2

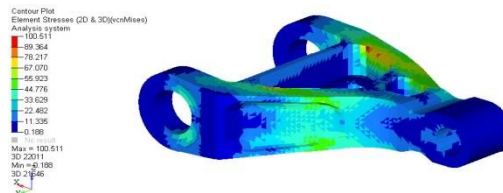


Figure 5.2: Vonmises stress for mild steel reference design.

Aluminium T6 Alloy

Even though the strength to weight ratio of Mild steel material is considered to be suitable for lower control arm in the past, for future control arms even better alternatives are being researched. One possible alternative in this respect is Aluminium T6 alloy. AluminiumT6 alloy is prescribed as the control arm material in the place of Mild steel. The displacement and stress results for this case are shown in figures 6.3 and 6.4 respectively. As usual, the maximum displacement occurred at free end. It is found that the maximum displacement of the control arm is lesser when AluminiumT6 alloy is used compared to the Mild steel lower control arm (see figures7.3 and7.4).

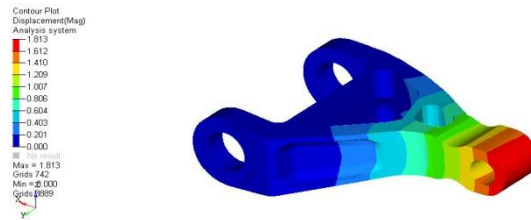


Figure 5.3: Displacement for aluminium-T6 design.

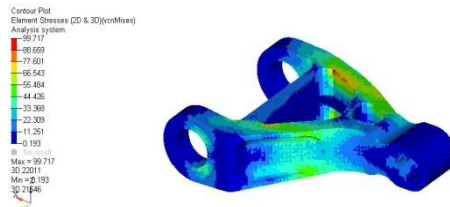


Figure 5.4: Vonmises stress for aluminium-T6 design

OPTIMIZED MODEL MILD STEEL

After completion of topology optimization First simulation is performed by taking the material of the control arm to be mild steel. From the fig6.5 it is clear that maximum displacement occurs at the free end. The maximum displacement of mild steel material is 0.609mm

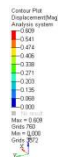


Figure 5.5: Displacements for mild steel optimize model design.

The optimized design is having the less stress when compare with the existing design as shown in Figure6.6. The vonmises stress of the optimized model is 63.527mm.

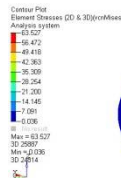


Figure 5.6: Vonmises stresses for mild steel optimize model design.

Aluminium T6 Alloy

The lower control arm behaves like a cantilever beam at the one hole side is fixed and two holes side is free so the maximum displacement is occurred at the one hole side as shown in fig6.7 The displacement of optimized model is 1.026mm.

International Journal of Innovative Research in Science, Engineering and Technology

(An ISO 3297: 2007 Certified Organization)

Website: www.ijirset.com

Vol. 6, Issue 6, June 2017

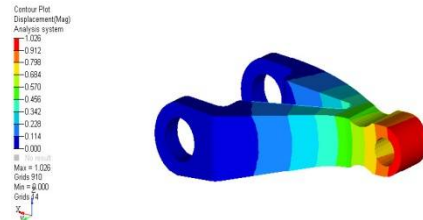


Figure 5.7: Displacement for aluminium-T6 optimize model design

For cantilever beam the maximum bending stresses is developed at fixed support. The von Mises stress distribution of lower control arm is shown in the figure6.8. The maximum displacement of lower control arm is 62.940mm.

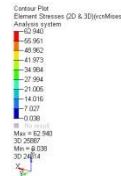


Figure 5.8: Vonmises stresses for aluminium-T6 optimize model design.

Discussion of Structural Analysis

The results of the structural analyses conducted for four different cases are summarized here. The maximum von Mises stresses and maximum displacements for each of two materials are as shown in the table 6.1, and they are also graphically presented in graph6.1 and6.2 respectively.

Final results

Materials	Base design		Optimized design	
	Displacement (mm)	Vonmises Stress (MPa)	Displacement (mm)	Vonmises Stress (MPa)
Mild steel	0.618	100.51	0.609	63.527
Al-T6	1.813	99.717	1.026	62.94

Table: Results obtained from the static structural analysis

Comparison of Stress

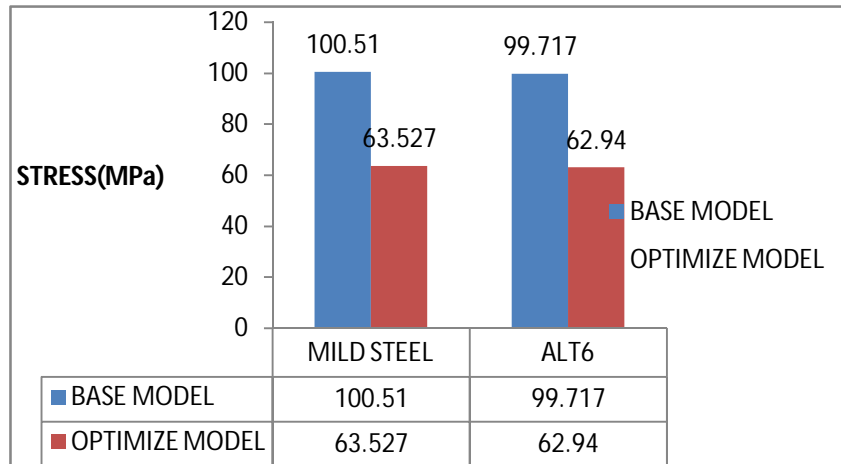
As was discussed already the comparison of the maximum stress across the four different cases considered here see Table6.1 shows that AluminiumT6 alloy after optimization gives least maximum stress while mild steel before optimization gives highest maximum stress. However, considering the weight of the lower control arm, AluminiumT6 alloy gives the least weight with the choice of given its low density.

International Journal of Innovative Research in Science, Engineering and Technology

(An ISO 3297: 2007 Certified Organization)

Website: www.ijirset.com

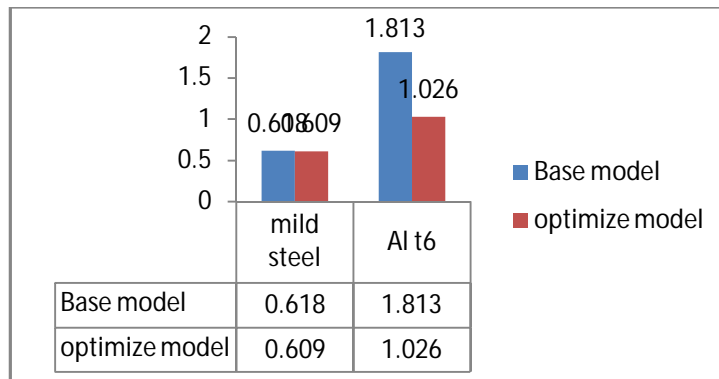
Vol. 6, Issue 6, June 2017



Graph 5.1: Von mises stress for base model and optimize model

Comparison of Displacement

A comparison of maximum deflection in all the cases considered here shows that AluminiumT6 alloy before optimization gives largest deflection. Also, Mild steel is having the less displacement because of its density.



Graph 5.2: Displacement for base model and optimize model

MODAL ANALYSIS

In this analysis, we determine the vibration characteristics and it is also used to calculate the natural frequencies at corresponding mode shapes. Various mode extraction methods are available. The required boundary conditions are, two holes was fixed in all degrees of freedom and the material properties was given for extracting the first three mode shapes of control arm are shown below.

Mode Shapes of existing model – Mild steelModel

The different mode shapes and its natural frequencies of the base model with mild steel are shown in Figures 6.9 – 6.11.

International Journal of Innovative Research in Science, Engineering and Technology

(An ISO 3297: 2007 Certified Organization)

Website: www.ijirset.com

Vol. 6, Issue 6, June 2017

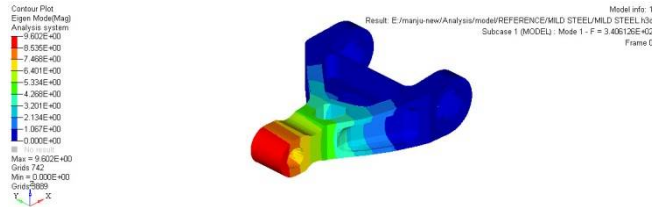


Figure 5.9: Mode-I for mild steel reference design.

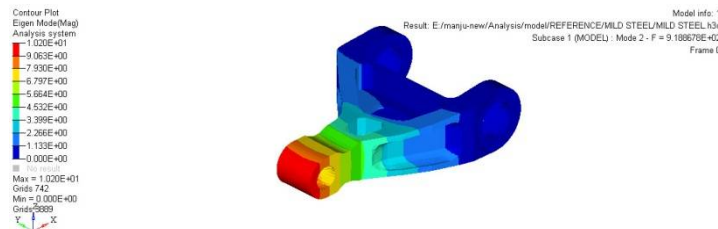


Figure 5.10: Mode-II for mild steel reference design.

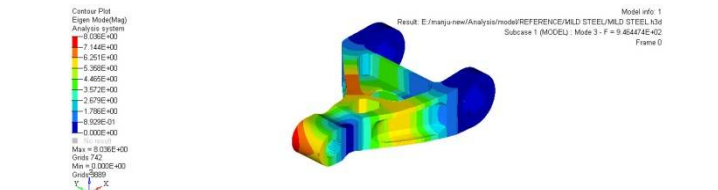


Figure 5.11: Mode-III for mild steel reference design.

Mode Shapes of existing model – aluminium-T6

The different mode shapes and its natural frequencies of the base model with aluminium –T6 are shown in Figures 6.12 – 6.14.

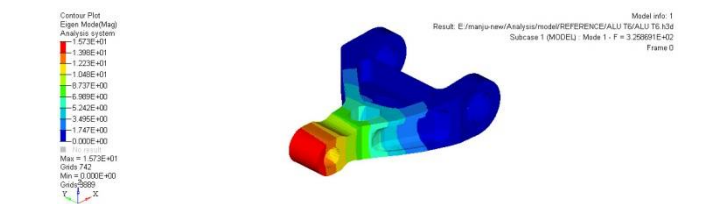


Figure 5.12: Mode-I for aluminium-T6 design

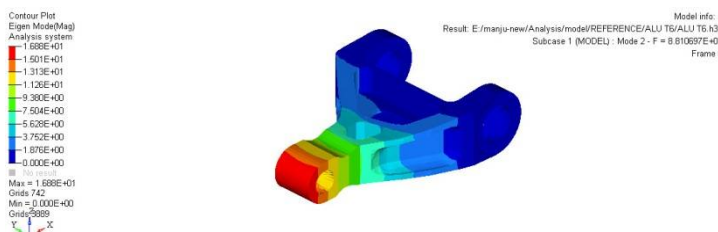


Figure 5.13: Mode-II for aluminium-T6 design

International Journal of Innovative Research in Science, Engineering and Technology

(An ISO 3297: 2007 Certified Organization)

Website: www.ijirset.com

Vol. 6, Issue 6, June 2017

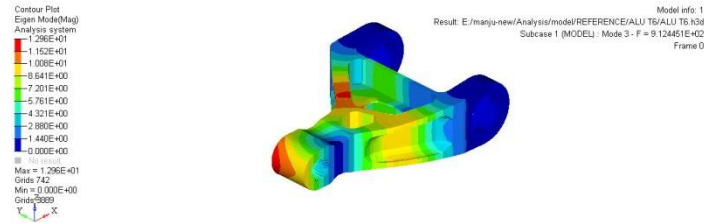


Figure 5.14: Mode-III for aluminium-T6 design

Mode shapes of optimized model – Mild steel

The different mode shapes and its natural frequencies of the Optimize model with Mild steel are shown in Figures 6.15 – 6.17.

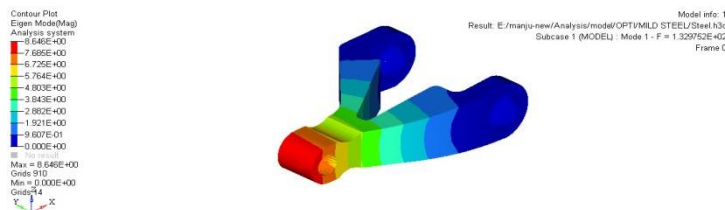


Figure 5.15: Mode-I for mild steel optimize model design

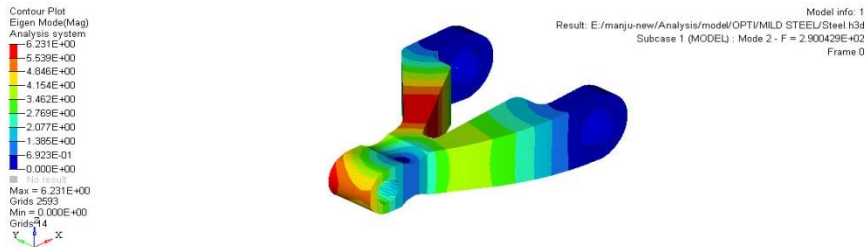


Figure 5.16: Mode-II for mild steel optimize model design

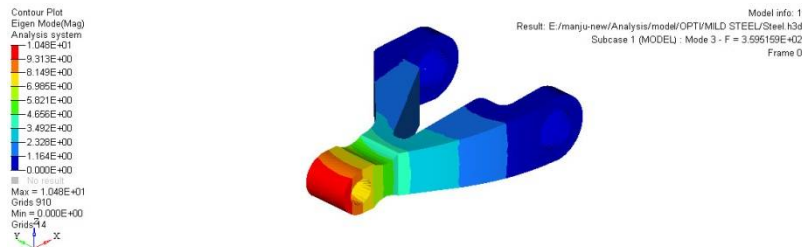


Figure 5.17: Mode-III for mild steel optimize model design

Mode shapes of optimized model-aluminium-T6

The different mode shapes and its natural frequencies of the Optimize model with aluminium –T6 are shown in Figures 6.18 – 6.20.

International Journal of Innovative Research in Science, Engineering and Technology

(An ISO 3297: 2007 Certified Organization)

Website: www.ijirset.com

Vol. 6, Issue 6, June 2017

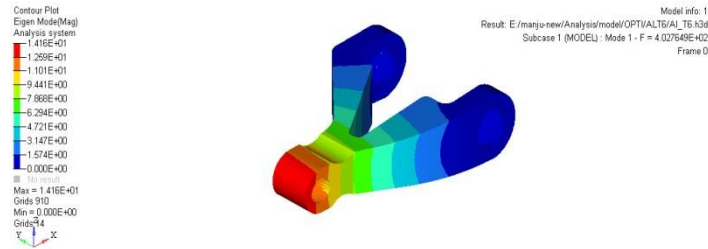


Figure : Mode-I for aluminium-T6 optimize model design.

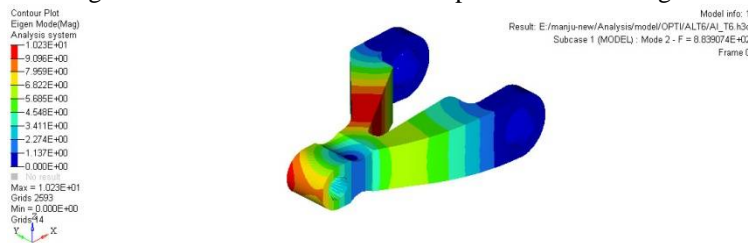


Figure: Mode-II for aluminium-T6 optimize model design.

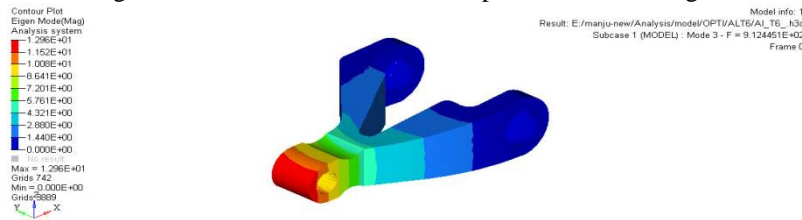


Figure: Mode-III for aluminium-T6 optimize model design.

Modal analysis results

Materials	Base design			Optimized design		
	Mode-1	Mode-2	Mode-3	Mode-1	Mode-2	Mode-3
Mild steel	3.406	9.188	9.464	1.329	2.900	3.595
Al-T6	3.258	8.810	9.124	4.027	8.839	9.123

Table : Results obtained from modal analysis

Graph:

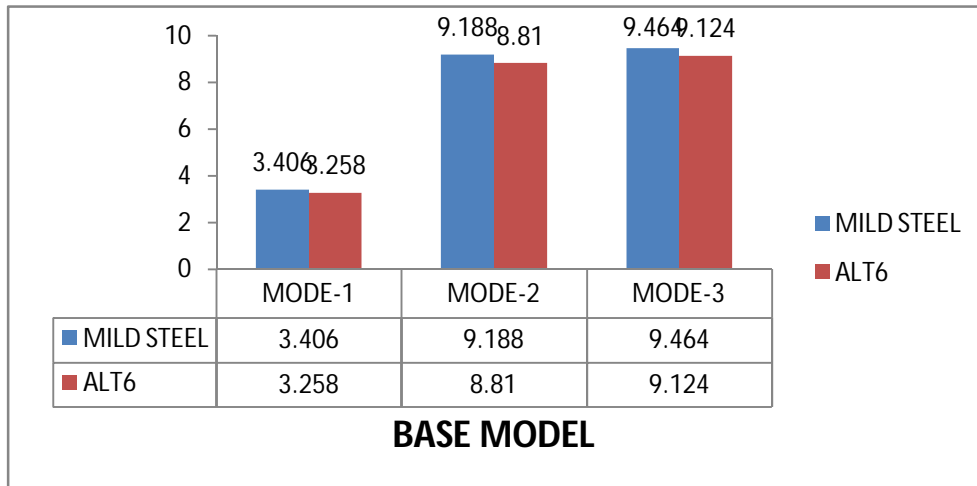
Based on the above results we draw the graph between mild steel alt6 model by comparing for base model frequencies as shown in below.

International Journal of Innovative Research in Science, Engineering and Technology

(An ISO 3297: 2007 Certified Organization)

Website: www.ijirset.com

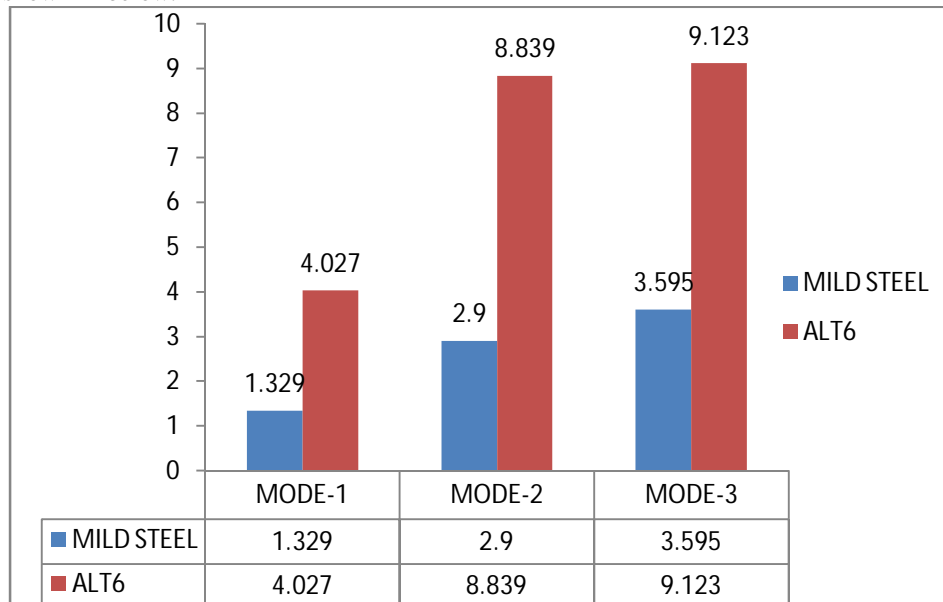
Vol. 6, Issue 6, June 2017



Graph : Frequency modes for base model

Graph:

Based on the above results we draw the graph between mild steel alt6 model by comparing for optimize model frequencies as shown in below.



Graph: Frequency modes for optimize model

Calculation of weight

The main objective of this study is to reduce the weight of the lower control arm using topology optimization and material optimization. In material optimization, it is necessary to introduce the materials having good mechanical properties like high strength to weight ratio. Mild steel and Aluminium alloy 7050T6 are used for this study to reduce the weight of the component. To calculate the weight of the model, use tool option displayed in Hyperworks. In tool option, click on the mass calculation option and select the all displayed elements to calculate the weight of the model as shown in Table

International Journal of Innovative Research in Science, Engineering and Technology

(An ISO 3297: 2007 Certified Organization)

Website: www.ijirset.com

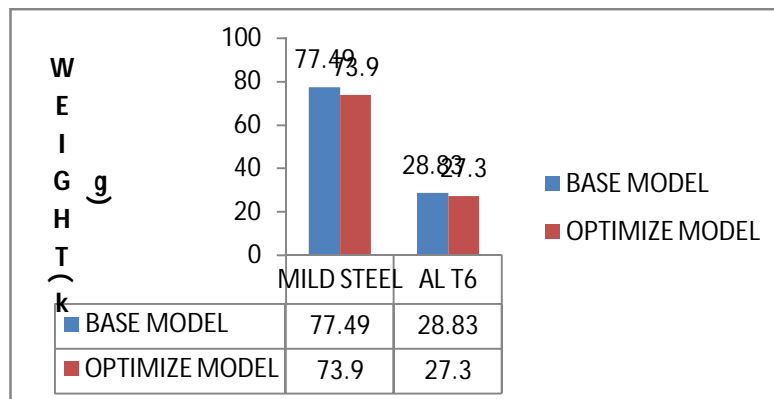
Vol. 6, Issue 6, June 2017

Materials	Base design weight in(kg)	Optimized design weight in(kg)
Mild steel	77.49	73.9
Al-T6	28.83	27.3

Table : Weight of the models with three different materials

Total weight reduction

$$\begin{aligned}
 &\text{Initial Weight of the component} &&= 77.49 \text{ Kg} \\
 &\text{Weight of the optimized model after material optimization} &&= 27.3 \text{ kg} \\
 \text{Total weight reduction} &= \frac{\text{Initial weight} - \text{Final weight}}{\text{Initial weight}} \\
 &= \frac{77.49 - 27.3}{77.49} \\
 \text{Percentage of total weight Reduction} &= 64.76\%
 \end{aligned}$$



Graph: Weight optimization for base model and optimize model

From the Graph, it is found the weight of the optimized model with aluminium-T6 is very less compared to mild steel. Hence the optimized model with aluminium-T6 is well suited for automobile applications.

International Journal of Innovative Research in Science, Engineering and Technology

(An ISO 3297: 2007 Certified Organization)

Website: www.ijirset.com

Vol. 6, Issue 6, June 2017

V.CONCLUSION AND FUTURE WORK

In this study, topology optimization approach is presented to create a new design of a lower control arm. Comparison between the existing model and optimized model is done in terms of stress, weight and the performance of the component. In this study, weight reduction of lower control arm is taken into consideration without varying the performance of the component. Firstly the process of the topology optimization involves the material distribution, which resulted that the weight of the existing industrial component is reduced to % of its total weight. The lower control arm has further undergone weight reduction using the different materials through the usage of ALTAIR OPTISTRUCT SOFTWARE. The obtained results states that % of weight reduction is done to the component. In this paper we have seen that the weight of the component is reduced to 64% by using optimized Aluminium Alloy 7075 T6 material made component. The future scope of this work focuses on the cost reduction of the material without varying the weight of the component. After the careful analysis of the better material the product is further undergone to topology optimization using Hyperworks software. The manufacturability of the component is been analyzed using the ALTAIR OPTISTRUCT and Optistruct analysis. Based on the results in this study, we proposed that the optimized model with Aluminium alloy 7075 T6 is best suited for the lower control arm.

REFERENCES

1. "Structural Design Method of a Control Arm with Consideration of Strength" By Jong-Kyu Kim 9th WSEAS Int. Conference on Applied Computer and Applied Computational Science Issue ISSN: 1790-5117.
2. "Met model-based optimization of a control arm considering strength and durability performance" by Xue Guan Song 2010 ELSEVIER journals Issue ISSN 976-980.
3. "Design and Optimization of Sheet Metal Control Arm for Independent Suspension System" by Nagarjuna.P October 2012 IJERA journal ISSN: 2248-9622.
4. "Design Analysis and Simulation of Double Wishbone Suspension System" by Vivekananda June 2014 IJME journal Volume 2 Issue 6
5. "Design of Electro-Hydraulic Active Suspension System for Four Wheel Vehicles" by Hemanth.D April 2014 IJETAE journal Volume 4 Issue 4 ISSN 2250-2459, ISO 9001
6. "Finite Element Analysis and Topology Optimization of Lower Arm of Double Wishbone Suspension using RADIOSS and Optistruct" by Vinayak Kulakarni May 2014 IJSR journal Volume 3 Issue 5 ISSN: 2319-7064
7. "Modelling and Finite Element Analysis of Double Wishbone Suspension" by Amol Patil April 2014 IJIRSET journal Volume 3 Issue 4 ISSN: 2319-8753
8. "Finite Element Analysis and Topography Optimization of Lower Arm of Double Wishbone Suspension Using Abacus and Optistruct" by Sagar Darge July 2014 IJERA journal volume 4 Issue 7 ISSN: 2248-9622
9. "Dynamic Structure Optimization Design of Lower Control Arm Based on ESL" by Songlin November 2012RJASET journal Volume 4 ISSN: 2040-7467